In memory of T. A. Stephenson

Gold–Boron Chemistry. Part 1. Synthetic, Structural, and Spectroscopic Studies on the Compounds [5,6-μ-(AuPR$_3$)-*nido*-B$_{10}$H$_{13}$] (R = cyclo-C$_6$H$_{11}$ or C$_6$H$_4$Me-2)†

Andrew J. Wynd, Alistair J. McLennan, David Reed, and Alan J. Welch *
Department of Chemistry, University of Edinburgh, Edinburgh EH9 3JJ

The new Class 2 gold–boron compounds [5,6-μ-(AuPR$_3$)-*nido*-B$_{10}$H$_{13}$] (**1a**; R = cyclo-C$_6$H$_{11}$; **1b**, R = C$_6$H$_4$Me-2) have been prepared by the reaction between [AuMe(PR$_3$)] and B$_{10}$H$_{14}$ in CH$_2$Cl$_2$. Compound (**1a**) is also afforded by reaction between [AuCl{P(C$_6$H$_{11}$)$_3$}] and [B$_{10}$H$_{13}$]$^-$. The exact mechanism of the first reaction is unclear, but probably proceeds *via* sequential oxidative addition and reductive elimination. Crystallographic analyses of compounds (**1**) show the expected decaborane-like geometry. There is some evidence of an intramolecular interaction between Au and the B(9)–H–B(10) bridge system. A thorough n.m.r. study of (**1b**) was undertaken, including an ^{11}B(COSY) experiment which allowed almost complete assignment of the ten inequivalent B atoms in the molecule.

There is continuing interest in the synthesis and characterisation of new metallaboranes and carbametallaboranes,[1–6] and important accompaniments to these experimental studies have been the recognition of simple structural patterns and statements of the associated electron-counting principles which serve to underpin the subject.[7]

Transition-metal derivatives of boranes and carbaboranes are now known for an impressive range of metals, but there are relatively few examples involving the Group 1B elements Cu, Ag, and Au. We find it convenient to divide the Group 1B derivatives according to structure type. Class 1 refers to those species in which the Group 1B element resides in a polyhedral vertex[6,8–14] whilst Class 2 refers to those in which the metal atom bridges a polyhedral edge.[15–20] A final group, Class 3, is that in which the polyhedron and Group 1B element are simply connected *via* a single two-centre two-electron bond.[21]

We recognise that some examples of Class 1 Group 1B metallaboranes may be contentious. Thus, for example, for [(Ph$_3$P)$_2$CuB$_3$H$_8$][9,10] it is a moot point whether or not one regards the Cu atom to be an integral part of the polyhedron. Doing so, one recognises that this species is simply a metallaborane derived from B$_4$H$_{10}$. Alternatively one might argue that the relationship between [(Ph$_3$P)$_2$CuB$_3$H$_8$] and [B$_3$H$_8$]$^-$ [22,23] is no more than that between [Cu$_2$B$_{10}$H$_{10}$][24] and [B$_{10}$H$_{10}$]$^{2-}$, *i.e.* covalent bonding between an *exo*-polyhedral B–H electron pair and the metal atom, in much the same way as one regards agostic M/C–H bonding in organometallic complexes.[25] For the present purposes we will regard molecules such as [(Ph$_3$P)$_2$CuB$_3$H$_8$] as Class 1 metallaboranes.

One of the many successes of the isolobal analogy developed by Hoffmann[26] is the popularity of the replacement of μ-H atoms in transition-metal cluster compounds by the (isolobal) {μ-AuPR$_3$} fragment, affording species that are frequently more stable and generally more readily analysed by *X*-ray crystallography.[27] Given that well known analogies exist between the electronic and consequent geometric structures of polyhedral boron hydrides and low-valent transition-metal clusters,[28] and that the *nido*, *arachno*, and *hypho* families of the former frequently contain several μ-H functions,[29] we became interested in the potential multiple replacement of H bridges in boranes by {AuPR$_3$} fragments, with the additional possibility of products containing gold–gold bonds.

This first paper in this series is concerned with species of the type [5,6-μ-(AuPR$_3$)-*nido*-B$_{10}$H$_{13}$] (**1**), in which a single μ-H atom of B$_{10}$H$_{14}$ is isolobally substituted. Some aspects of this work have been communicated previously.[30]

Experimental

Syntheses.—Standard Schlenk-tube techniques were used throughout, with all solvents thoroughly dried and distilled under N$_2$ before use. N.m.r. spectra were recorded at room temperature on JEOL FX 60 Q (^{31}P) and Brucker WP 200 SY (^{1}H) and WH 360 (^{1}H, ^{11}B) spectrometers, the last fitted with an Aspect 3000 computer. Chemical shifts are relative to external SiMe$_4$ (^{1}H), 85% H$_3$PO$_4$ (^{31}P), and BF$_3$·OEt$_2$ (^{11}B), positive values to high frequency. Techniques for recording ^{1}H-{^{11}B} and ^{11}B(COSY) spectra have been described previously.[31] I.r. spectra were recorded as KBr discs or as CH$_2$Cl$_2$ solutions on a Perkin-Elmer 598 spectrophotometer. Microanalyses were by the departmental service.

[AuX(PR$_3$)] (X = Cl *or* Me; R = *cyclo*-C$_6$H$_{11}$ *or* C$_6$H$_4$-Me-2). The known[32] species [AuCl{P(C$_6$H$_{11}$)$_3$}] was prepared by direct reaction[33] between HAuCl$_4$ and P(C$_6$H$_{11}$)$_3$ in absolute ethanol[34] and its purity checked by C and H microanalysis and by n.m.r. spectroscopy [^{31}P-{^{1}H} (CD$_2$Cl$_2$), δ 53.9 (s) p.p.m.]. The compound [AuCl{P(C$_6$H$_4$Me-2)$_3$}] was synthesised analogously as colourless *crystals* in 91% yield (Found: C, 46.9; H, 3.90. C$_{21}$H$_{21}$AuClP requires C, 46.9; H, 3.90%); ^{31}P-{^{1}H} (CDCl$_3$), δ 8.2 (s) p.p.m. Methylation of the phosphine gold chlorides using LiMe in Et$_2$O[35] afforded white *crystals* of [AuMe{P(C$_6$H$_{11}$)$_3$}] [91% (Found: C, 45.7; H, 7.25. C$_{19}$H$_{36}$AuP requires C, 46.3; H, 7.35%); ^{31}P-{^{1}H} (CD$_2$Cl$_2$), δ 59.9 (s) p.p.m.] and [AuMe{P(C$_6$H$_4$Me-2)$_3$}] [68% (Found: C, 50.2; H, 4.50. C$_{22}$H$_{24}$AuP requires C, 51.2; H, 4.70%); ^{31}P-{^{1}H} (CD$_2$Cl$_2$), δ 37.0 (s) p.p.m.].

---

† 5,6-μ-[Tri(cyclohexyl)phosphine]aurio- and 5,6-μ-[tri(*o*-tolyl)-phosphine]aurio-*nido*-decaborane, respectively.

Supplementary data available: see Instructions for Authors, *J. Chem. Soc., Dalton Trans.*, 1987, Issue 1, pp. xvii—xx.

$[5,6\text{-}\mu\text{-Au}\{P(C_6H_{11})_3\}\text{-}nido\text{-}B_{10}H_{13}]$ (**1a**). To a stirred solution of $[AuMe\{P(C_6H_{11})_3\}]$ (0.7715 g, 1.567 mmol) in CH_2Cl_2 (10 cm^3) was added, dropwise, a solution of $B_{10}H_{14}$ (0.1913 g, 1.567 mmol) in CH_2Cl_2 (10 cm^3 and 15 cm^3 washings). A bright yellow solution was quickly formed, followed by gas evolution and the deposition of a white precipitate. The solid product was filtered off and washed with 2 × 5 cm^3 aliquots of ice-cold CH_2Cl_2. The volume of the combined filtrate and washings was reduced *in vacuo* and cooled to −30 °C to afford a second crop of crystalline solid, subsequently recovered. The combined solid product was purified by recrystallisation from CH_2Cl_2, affording colourless *crystals* (0.703 g, 75%) (Found: C, 35.7; H, 7.70. $C_{18}H_{46}AuB_{10}P$ requires C, 36.1; H, 7.75%); $\nu_{max.}$(KBr) at 2 900, 2 844 (both C–H), 2 530br (B–H), 1 920—1 850vw (B–H–B), 1 440 (C–H), 1 000 (P–C), 510 (Au–P), 470w, and 385w (both Au–B) cm^{-1}. N.m.r.: $^{31}P\text{-}\{^1H\}$ (CD_2Cl_2), δ 68.9 (br); ^1H, δ 1.84 (br), 1.63 and 1.27 (br); $^{11}B\text{-}\{^1H\}$ ($CDCl_3$), δ 16.12 (1 B), 9.32 (1 B), 8.41 (1 B), 2.82 (1 B), 1.41 (1 B), −0.57 (2 B), −1.01 (1 B), −29.53 (1 B), and −35.63 (1 B); $^1H\text{-}\{^{11}B\}$ ($CDCl_3$), δ 5.05, 3.72, 3.50, 3.29, 3.17, 2.94, 2.90, 2.62, 0.64, 0.60 (all B–H), −0.13, −2.93, and −3.84 (all B–H–B) p.p.m.

Alternatively, to a freshly prepared,[36] stirred solution of $[NEt_3H][B_{10}H_{13}]$ (0.195 mmol) in CH_2Cl_2 (15 cm^3) was added, dropwise, $[AuCl\{P(C_6H_{11})_3\}]$ (0.100 g, 0.195 mmol) in the same solvent (25 cm^3). The resultant bright yellow solution was stirred for *ca.* 4 h at ambient temperature. After removal of solvent *in vacuo*, addition of CH_2Cl_2 afforded a yellow solution and a white precipitate. The latter was identified as compound (**1a**) by $^{31}P\text{-}\{^1H\}$ n.m.r. and microanalysis. Yield 0.060 g, 51%.

$[5,6\text{-}\mu\text{-Au}\{P(C_6H_4Me\text{-}2)_3\}\text{-}nido\text{-}B_{10}H_{13}]$ (**1b**). This was entirely analogous to the first preparation for compound (**1a**) except that the product was not deposited from CH_2Cl_2 until a concentrated solution was cooled (−30 °C). The product was washed with ice-cold hexane (2 × 5 cm^3) to afford very pale yellow *crystals* in 65% yield. Microanalytical results on a crystalline sample are consistent with the 1:1 solvate $[\{(C_6H_4Me\text{-}2)_3P\}AuB_{10}H_{13}]\cdot CH_2Cl_2$ (Found: C, 37.0; H, 5.10. $C_{21}H_{34}AuB_{10}P\cdot CH_2Cl_2$ requires C, 37.4; H, 5.15%); $\nu_{max.}$(CH_2Cl_2) at 2 905, 2 940 (both C–H), 2 550 (B–H), 1 590 (C–C), 1 450 (C–H), 1 010 (P–C), and 555 (Au–P) cm^{-1}. N.m.r. (CD_2Cl_2): $^{31}P\text{-}\{^1H\}$, δ 26.9 (br) p.p.m.; $^{11}B\text{-}\{^1H\}$ and $^1H\text{-}\{^{11}B\}$ chemical shifts are reported and assignments discussed in the Results and Discussion section.

Crystallographic Studies.—Diffraction-quality single crystals of compounds (**1a**) and (**1b**) were grown by solvent diffusion (CH_2Cl_2–n-hexane, 1:4) at −30 °C, and were studied at 291 and 273 K respectively on an Enraf-Nonius CAD4 diffractometer using graphite-monochromated Mo-K_α *X*-radiation, $\bar{\lambda}$ = 0.710 69 Å.

Crystal data. (**1a**), $C_{18}H_{46}AuB_{10}P$, $M = 598.6$, monoclinic, $a = 11.658\ 3(20)$, $b = 22.663(6)$, $c = 11.418(3)$ Å, $\beta = 118.061(16)°$, $U = 2\ 662$ Å^3, by the least-squares refinement of 25 centred reflections, $12 < \theta < 14°$, space group $P2_1/a$, $Z = 4$, $D_c = 1.493$ g cm^{-3}, $\mu(\text{Mo-}K_\alpha) = 55.8$ cm^{-1}, $F(000) = 1\ 192$.

(**1b**), $C_{21}H_{34}AuB_{10}P\cdot CH_2Cl_2$, $M = 707.5$, monoclinic, $a = 10.370(3)$, $b = 20.100(4)$, $c = 15.283(4)$ Å, $\beta = 106.782(23)°$, $U = 3\ 050$ Å^3, derived as above, $13 < \theta < 15°$, space group $P2_1/c$, $Z = 4$, $D_c = 1.541$ g cm^{-3}, $\mu(\text{Mo-}K_\alpha) = 50.6$ cm^{-1}, $F(000) = 1\ 348$.

Data collection and processing. (**1a**). ω—2θ Scans in 96 steps with ω scan-width 0.8 + 0.35tanθ. Variable scan speeds between 1.27 and 5.49° min^{-1}. 2 473 Unique data were measured ($1 < \theta < 20°$, $+h$ $+k$ $+l$ and $+h$ $+k$ $-l$) yielding 1 821 with $F > 5.0\sigma(F)$. No measurable crystal decay or detectable movement.

(**1b**). As above except scan speeds between 1.03 and 2.35° min^{-1}; 3 976 data ($\theta_{max.}$ 22°) of which 3 072 had $F > 2.0\sigma(F)$; crystal decayed by *ca.* 4% during experiment and correction applied.

Structure solution and refinement. (**1a**). Patterson synthesis for Au atom, and iterative full-matrix least-squares refinement and Δ*F* syntheses for P, B, and C atoms. Empirical absorption correction[37] applied after isotropic convergence. Ultimately Au, P, and B atoms allowed anisotropic thermal motion. Cyclohexyl hydrogen atoms set in idealised positions (C–H 1.08 Å) with an overall isotropic thermal parameter [0.044(7) Å^2 at convergence]. Weighting scheme $w^{-1} = [\sigma^2(F) + 0.000\ 117(F)^2]$, $R = 0.0426$, $R' = 0.0492$, $S = 1.190$. Data: variables, 10:1. Maximum and minimum electron-density residues 0.707 and −0.550 e Å^{-3}. Scattering factors for Au from ref. 38, those for P, B, C, and H being inlaid in SHELX 76.[39] Computer programs CADABS,[40] SHELX 76, DIFABS, CALC,[41] and ORTEP II.[42] Co-ordinates of refined atoms are given in Table 1.

(**1b**). Gold atom located by automatic direct methods[43] and P, B, C, and Cl atoms by subsequent iterative full-matrix least-squares refinement and Δ*F* syntheses. Empirical absorption correction applied after isotropic convergence. Ultimately Au, P, B, C, and Cl atoms allowed anisotropic thermal motion. Phenyl rings were constrained as rigid planar hexagons with fixed bond length (C–C 1.395 Å). Hydrogen atoms of the phenyl rings were set in idealised positions (C–H 1.08 Å) and refined with one overall thermal parameter, 0.062(10) Å^2 at convergence. Hydrogen atoms of the methyl groups and of the B_{10} cage could not be either satisfactorily located or modelled and remain absent. The dichloromethane solvate molecule involves one chlorine atom [Cl(2)] disordered over two positions (a and b) with occupancy factors of 0.430(13) and 0.570 at convergence. Weighting scheme $w^{-1} = [\sigma^2(F) + 0.000\ 773(F)^2]$, $R = 0.0519$, $R' = 0.0676$, $S = 1.191$. Data: variables = 10:1, with

Table 1. Fractional co-ordinates of refined atoms in compound (**1a**)

Atom	*x*	*y*	*z*
Au	0.192 61(6)	0.229 78(3)	0.422 62(6)
P	0.184 4(4)	0.138 77(18)	0.327 9(4)
C(11)	0.243 9(13)	0.081 1(7)	0.457 9(13)
C(12)	0.163 2(15)	0.082 9(7)	0.532 5(15)
C(13)	0.225 0(15)	0.038 7(8)	0.649 5(15)
C(14)	0.365 1(14)	0.050 2(8)	0.741 5(15)
C(15)	0.444 4(15)	0.048 3(7)	0.664 7(14)
C(16)	0.391 0(13)	0.089 6(7)	0.551 2(13)
C(21)	0.023 6(13)	0.118 9(6)	0.198 2(13)
C(22)	−0.087 8(13)	0.150 0(7)	0.221 3(14)
C(23)	−0.221 7(14)	0.139 6(7)	0.102 5(15)
C(24)	−0.246 7(16)	0.075 3(8)	0.080 6(16)
C(25)	−0.145 2(14)	0.042 3(7)	0.067 7(15)
C(26)	−0.006 0(14)	0.051 3(7)	0.181 9(14)
C(31)	0.291 7(13)	0.138 6(6)	0.249 6(13)
C(32)	0.259 6(13)	0.189 1(7)	0.155 7(14)
C(33)	0.361 5(14)	0.192 9(7)	0.101 0(14)
C(34)	0.372 4(16)	0.133 9(7)	0.041 9(15)
C(35)	0.400 4(15)	0.084 3(7)	0.138 6(15)
C(36)	0.298 9(14)	0.079 9(7)	0.189 9(15)
B(2)	0.209 8(17)	0.375 4(8)	0.557 6(18)
B(5)	0.155 0(18)	0.300 7(8)	0.536 1(17)
B(1)	0.225 4(17)	0.333 2(8)	0.701 8(17)
B(3)	0.359 9(22)	0.378 6(10)	0.717 2(23)
B(10)	0.280 6(21)	0.260 3(11)	0.709 3(19)
B(4)	0.391 2(19)	0.313 8(12)	0.812 6(21)
B(7)	0.363 5(20)	0.371 3(10)	0.564 2(22)
B(6)	0.237 7(20)	0.330 1(9)	0.450 0(21)
B(9)	0.462 3(20)	0.264 4(14)	0.751 2(22)
B(8)	0.486(3)	0.335 0(11)	0.741(3)

Table 2. Fractional co-ordinates of refined atoms in compound (**1b**)

Atom	*x*	*y*	*z*
Au	0.541 24(4)	0.552 46(2)	0.211 55(3)
P	0.736 3(3)	0.529 03(13)	0.326 00(18)
C(16)	0.952 1(5)	0.445 9(3)	0.336 2(5)
C(15)	1.0157	0.3853	0.3322
C(14)	0.9397	0.3272	0.3104
C(13)	0.8000	0.3296	0.2926
C(12)	0.7364	0.3903	0.2965
C(11)	0.8124	0.4484	0.3184
C(121)	0.583 9(12)	0.387 8(6)	0.281 4(9)
C(26)	0.747 7(7)	0.474 5(3)	0.494 2(5)
C(25)	0.7217	0.4721	0.5788
C(24)	0.6543	0.5246	0.6062
C(23)	0.6130	0.5795	0.5491
C(22)	0.6390	0.5818	0.4646
C(21)	0.7064	0.5294	0.4371
C(221)	0.590 1(13)	0.644 8(6)	0.406 5(9)
C(36)	0.928 3(7)	0.621 7(4)	0.414 3(4)
C(35)	1.0321	0.6673	0.4210
C(34)	1.0777	0.6801	0.3452
C(33)	1.0194	0.6474	0.2628
C(32)	0.9156	0.6018	0.2561
C(31)	0.8701	0.5889	0.3319
C(321)	0.855 5(15)	0.565 9(6)	0.162 8(8)
B(1)	0.258 8(15)	0.668 2(8)	0.086 7(10)
B(2)	0.240 4(15)	0.588 5(8)	0.032 7(10)
B(3)	0.267 9(15)	0.659 6(8)	−0.027 7(10)
B(4)	0.362 0(16)	0.724 4(8)	0.042 3(10)
B(5)	0.335 2(14)	0.596 0(8)	0.146 9(10)
B(6)	0.378 5(15)	0.541 2(7)	0.071 3(11)
B(7)	0.350 8(14)	0.582 1(8)	−0.032 5(10)
B(8)	0.433 6(16)	0.676 9(8)	−0.030 5(11)
B(9)	0.531 1(16)	0.702 3(8)	0.080 3(12)
B(10)	0.425 7(16)	0.685 4(8)	0.155 4(11)
C(sol)	0.128 3(23)	0.336 9(12)	0.116 3(19)
Cl(1)	0.245 5(7)	0.297 5(5)	0.211 8(5)
Cl(2a)	0.192 2(21)	0.407 0(14)	0.133 6(16)
Cl(2b)	0.164 7(10)	0.302 7(5)	0.014 8(7)

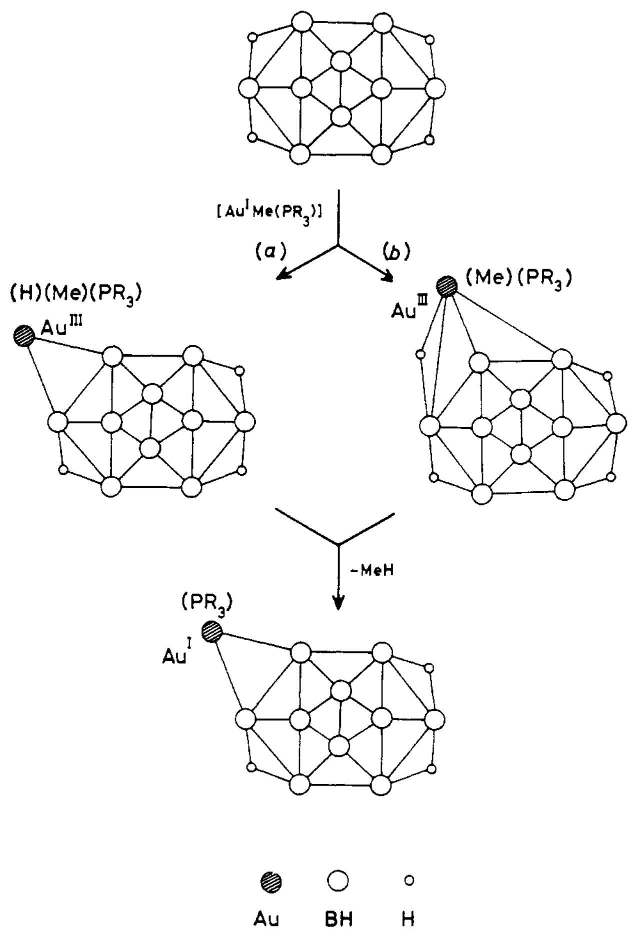

Scheme. Possible routes to compounds (**1**) from $B_{10}H_{14}$ and [AuMe(PR$_3$)] *via* (*a*) a terminal gold hydride intermediate, and (*b*) a bridging gold hydride intermediate

maximum and minimum electron-density residues of 2.817 and −1.487 e Å^{-3} respectively. Co-ordinates of refined atoms are given in Table 2.

Results and Discussion

Syntheses and Mechanism.—Dropwise addition of a solution of [AuMe(PR$_3$)] to $B_{10}H_{14}$ affords the air-stable colourless or pale yellow Class 2 crystalline compounds [5,6-μ-(AuPR$_3$)-*nido*-$B_{10}H_{13}$] (**1a**, R = cyclo-C_6H_{11}; **1b**, R = C_6H_4Me-2) in reasonable yields. If the reaction is performed as above (**1a**) or (**1b**) is the only isolable product. If, however, $B_{10}H_{14}$ is added dropwise to 1 equivalent of [AuMe{P(C_6H_{11})$_3$}] at least two other species may be isolated,[44] although (**1a**) is still the major product. As the following crystallographic and spectroscopic studies show, compounds (**1**) are the first proven examples[6] of the [$B_{10}H_{13}$]$^-$ unit acting as an η^2-ligand to a metal centre, although in [{Cd($B_{10}H_{12}$)(OEt$_2$)$_2$}$_2$][45] the cage functions as a bis η^2-ligand.

Alternatively, (**1a**) may be synthesised directly from [AuCl{P(C_6H_{11})$_3$}] by its reaction with [NEt$_3$H][$B_{10}H_{13}$]. In this preparation other species are also produced even if the chloride is added slowly to 1 equivalent of the ion. Amongst these additional products [NEt$_3$H]Cl has been identified. Similar reactions using [AuCl(PPh$_3$)] and [AuCl(PEt$_3$)] did not afford analogues of (**1**) in detectable amounts, but instead produced orange-yellow compounds which are currently being studied.[44]

The isolation of compounds (**1a**) and (**1b**) from $B_{10}H_{14}$ and [AuMe(PR$_3$)] appears to depend upon the large Tolman cone angles[46] of the phosphines [P(C_6H_{11})$_3$, 170°; P(C_6H_4Me-2)$_3$, 194°]. We have shown[30] that analogous reactions using [AuMe(PPh$_3$)] or [AuMe(PEt$_3$)] (phosphine cone angles 145 and 132° respectively) afford the unique 'triple clusters' [($B_{10}H_{12}$Au)(AuPR$_3$)$_4$(Au$B_{10}H_{12}$)] as the only isolable gold–boron species, although it is probable that these arise *via* the initial formation of compounds analogous to (**1a**) and (**1b**). We are actively pursuing alternative routes to these analogues that do not allow their further reaction.

When [AuMe(PR$_3$)] (R = C_6H_{11} or C_6H_4Me-2) is added to $B_{10}H_{14}$ a bright yellow solution is first formed, suggesting initial oxidation of the gold atom. As this solution then decolourises, gas evolution is noted. To obtain further information on the possible mechanism(s) by which (**1a**) and (**1b**) are produced we have followed the reaction between [AuMe{P(C_6H_{11})$_3$}] and $B_{10}H_{14}$ in CD_2Cl_2 by variable-temperature ^{1}H and ^{31}P-{^{1}H} n.m.r. spectroscopy, and between [AuMe{P(C_6H_4Me-2)$_3$}] and $B_{10}H_{14}$ in CD_2Cl_2 by variable-temperature ^{1}H, ^{1}H-{^{11}B}, and ^{11}B n.m.r. spectroscopy. In no case could any signals assignable to species other than the appropriate precursors or product be observed.

We cannot, therefore, authoritatively comment on the precise mechanistic details of the formation of compounds (**1**) from the methyl(phosphine)gold compounds at this stage. The bench observations are consistent with initial oxidative addition followed by reductive elimination, the simplest equation for the reactions suggesting elimination of methane. Two possible re-

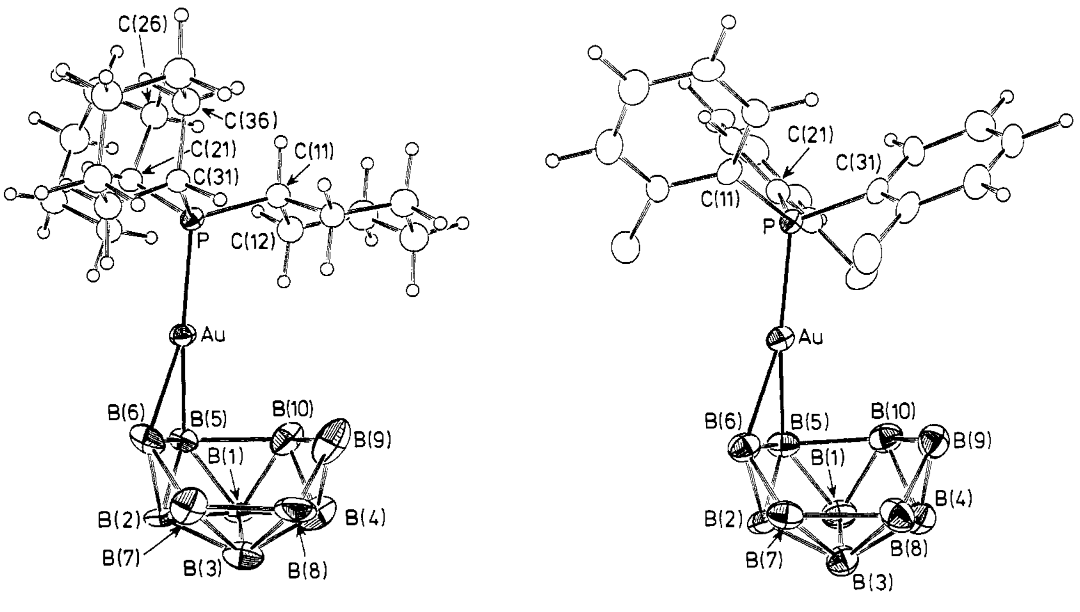

(*a*) (*b*)

Figure 1. Perspective views of (*a*) compound (**1a**) and (*b*) (**1b**). Non-hydrogen atoms represented by 30% probability ellipsoids, and H atoms given an artificial radius of 0.1 Å

action mechanisms are outlined in the Scheme. One possibility, (*a*) involves insertion of [AuMe(PR$_3$)] into the B(5)–H–B(6) bond of $B_{10}H_{14}$ to afford the transient species [5,6-μ-(H)Au^{III}(Me)(PR$_3$)-$B_{10}H_{13}$]. This compound would be unique in having a terminal Au–H function. Irreversible intramolecular reductive elimination of MeH would then give (**1a**) or (**1b**) as appropriate. Presumably the H and Me ligands of the intermediate would be mutually *cis*, *i.e.* H or Me *trans* to B–B. It should be noted that the oxidative insertion of a {Pt^0(PEt$_3$)$_2$} fragment into B–H–B bonds of 2,3-$C_2B_4H_8$, 2,3-Me$_2$-2,3-$C_2B_4H_6$, and 2-CB_5H_9 produces species in which the terminal hydride ligand is *trans* to the metal-bonded B–B edge.[47] An alternative intermediate species, route (*b*), might involve the Au^{III} atom as a vertex in an expanded polyhedron and have an Au–H–B bridge. The precise cage geometry of such an intermediate would depend upon the skeletal electron contribution of the metal vertex, and by analogy with recent studies[44] we suggest an *arachno* 11-vertex architecture for this species. The intermediate would afford (**1**) by eliminating methane and undergoing vertex-to-bridge slipping of the metal fragment in a manner essentially the reverse of that which we have suggested could occur in the formation of bis(cage)gold products.[44] The attraction of this second route is that although gold-hydride species are still rare, all proven examples to date have involved heteronuclear Au–H–X fragments.[48,49]

The proposed oxidative-addition step in the reaction between [AuMe(PR$_3$)] and $B_{10}H_{14}$ outlined in the above mechanisms may be contrasted with the report[50] that B_2H_6 *reduces* [AuCl(PPh$_3$)] to [Au$_{55}$(PPh$_3$)$_{12}$Cl$_6$] in benzene solution.

Structural Studies.—Figure 1(*a*) and (*b*) present common views of compounds (**1a**) and (**1b**) respectively, and Tables 3 and 4 list the derived internuclear distance and interbond angle information for each. Both species crystallise as monomers separated by nothing more than normal van der Waals contacts. In the crystal of (**1b**) there is additionally a (partially disordered) molecule of CH_2Cl_2, but this makes no close approach either to (**1b**) or to other solvate molecules.

Compounds (**1**) have decaborane-like cage structures in which the μ-AuPR$_3$ unit simply replaces the 5,6-μ-H atom of $B_{10}H_{14}$. The effect of this isolobal replacement on the geometry of the borane cage appears to be minimal. With Edinburgh software[41] we can quantify the extent to which two similar groups of atoms, located crystallographically, may be best fitted to each other. The refined root mean square (r.m.s.) misfit of the B_{10} cage of (**1a**) to that determined, very accurately,[51] for $B_{10}H_{14}$ (average of two crystallographically independent molecules) is only 0.080 Å. For (**1b**) the value is 0.049 Å. Equally, the optimised r.m.s. misfit between the B_{10} cages of (**1a**) and (**1b**) is 0.067 Å, and only 0.068 Å if Au and P atoms are also included.

Although the overall fit of the B_{10} polyhedra of compounds (**1**) with that of $B_{10}H_{14}$ is very good, a comparison of individual molecular parameters reveals some subtle differences. Thus, we note that the Au atoms of (**1a**) and (**1b**) bridge the B(5)–B(6) connectivity more asymmetrically than do the μ-H atoms of $B_{10}H_{14}$, although the direction of the asymmetry is the same [away from the low-connected atom, B(6)]. In (**1**) the average B(6)–Au bond length is 2.323 Å, whilst the average for B(5)–Au is 2.245 Å [in $B_{10}H_{14}$ average bond lengths are B(6,9)–(μ-H) 1.3485 and B(5,7,8,10)–(μ-H) 1.3250 Å]. This increased asymmetry is accompanied by unequal P–Au–B angles in (**1a**), the wider being to B(5) [this feature is not apparent in (**1b**)], and longer H-bridged B–B distances between B(9) and B(10) than between B(6)–B(7) or B(8)–B(9). Individually these features may be of little statistical significance, but taken together they are not inconsistent with some sort of weak interaction between the Au atom annd the B(9)–H–B(10) bridge system. Unfortunately the relative inaccuracies of the present structural studies of (**1a**) and (**1b**) preclude a more detailed discussion at this time. However, we plan to address this potentially interesting problem by a combined theoretical and highly accurate crystallographic study in the near future.

N.M.R. Studies on (**1b**).—The ^{11}B-{^{1}H} spectrum of (**1b**) (Figure 2) comprises eight signals with relative areas 1:1:1:1:1:3:1:1, and the ^{11}B spectrum (Figure 3) confirms

Table 3. Internuclear distances (Å) and interbond angles (°) in compound (**1a**)

Au–P	2.310(4)	C(21)–C(22)	1.606(22)	C(35)–C(36)	1.550(23)	B(1)–B(4)	1.80(3)
Au–B(5)	2.233(20)	C(21)–C(26)	1.562(22)	B(2)–B(5)	1.79(3)	B(3)–B(4)	1.76(3)
Au–B(6)	2.321(22)	C(22)–C(23)	1.530(23)	B(2)–B(1)	1.84(3)	B(3)–B(7)	1.77(3)
P–C(11)	1.850(16)	C(23)–C(24)	1.485(24)	B(2)–B(3)	1.84(3)	B(3)–B(8)	1.69(4)
P–C(21)	1.816(15)	C(24)–C(25)	1.463(25)	B(2)–B(7)	1.76(3)	B(10)–B(4)	1.76(3)
P–C(31)	1.848(15)	C(25)–C(26)	1.544(23)	B(2)–B(6)	1.75(3)	B(10)–B(9)	1.94(4)
C(11)–C(12)	1.539(22)	C(31)–C(32)	1.490(21)	B(5)–B(1)	1.83(3)	B(4)–B(9)	1.72(4)
C(11)–C(16)	1.547(21)	C(31)–C(36)	1.515(22)	B(5)–B(6)	1.80(3)	B(4)–B(8)	1.73(4)
C(12)–C(13)	1.550(24)	C(32)–C(33)	1.583(23)	B(5)–B(10)	2.04(3)	B(7)–B(6)	1.71(3)
C(13)–C(14)	1.492(24)	C(33)–C(34)	1.529(23)	B(1)–B(3)	1.81(3)	B(7)–B(8)	2.02(4)
C(14)–C(15)	1.546(23)	C(34)–C(35)	1.500(24)	B(1)–B(10)	1.76(3)	B(9)–B(8)	1.64(4)
C(15)–C(16)	1.478(22)						

P–Au–B(5)	159.7(5)	C(22)–C(21)–C(26)	107.4(12)	Au–B(5)–B(10)	89.6(10)	B(1)–B(4)–B(3)	61.3(13)
P–Au–B(6)	153.4(6)	C(21)–C(22)–C(23)	110.7(12)	B(1)–B(5)–B(10)	53.8(10)	B(1)–B(4)–B(10)	59.3(13)
B(5)–Au–B(6)	46.4(7)	C(22)–C(23)–C(24)	109.7(14)	B(2)–B(5)–B(1)	61.2(11)	B(3)–B(4)–B(8)	57.8(15)
Au–P–C(11)	109.7(5)	C(23)–C(24)–C(25)	114.5(15)	B(2)–B(5)–B(6)	58.3(11)	B(10)–B(4)–B(9)	67.8(15)
Au–P–C(21)	113.8(5)	C(24)–C(25)–C(26)	115.2(14)	B(10)–B(5)–B(6)	111.8(14)	B(9)–B(4)–B(8)	56.6(15)
Au–P–C(31)	109.9(5)	C(21)–C(26)–C(25)	108.3(13)	B(2)–B(1)–B(5)	58.3(10)	B(2)–B(7)–B(3)	62.8(13)
C(11)–P–C(21)	109.4(7)	P–C(31)–C(32)	110.4(10)	B(2)–B(1)–B(3)	60.5(12)	B(2)–B(7)–B(6)	60.4(13)
C(11)–P–C(31)	107.7(7)	P–C(31)–C(36)	114.4(11)	B(5)–B(1)–B(10)	69.4(12)	B(3)–B(7)–B(8)	52.5(13)
C(21)–P–C(31)	106.2(7)	C(32)–C(31)–C(36)	113.5(13)	B(3)–B(1)–B(4)	58.4(13)	B(6)–B(7)–B(8)	119.3(17)
P–C(11)–C(12)	109.2(10)	C(31)–C(32)–C(33)	110.2(13)	B(10)–B(1)–B(4)	59.2(13)	Au–B(6)–B(5)	64.2(9)
P–C(11)–C(16)	109.9(10)	C(32)–C(33)–C(34)	111.1(13)	B(2)–B(3)–B(1)	60.4(12)	Au–B(6)–B(7)	134.2(14)
C(12)–C(11)–C(16)	112.5(12)	C(33)–C(34)–C(35)	111.4(14)	B(2)–B(3)–B(7)	58.2(12)	B(2)–B(6)–B(5)	60.5(12)
C(11)–C(12)–C(13)	107.6(13)	C(34)–C(35)–C(36)	112.7(14)	B(1)–B(3)–B(4)	60.3(13)	B(2)–B(6)–B(7)	61.2(13)
C(12)–C(13)–C(14)	113.9(14)	C(31)–C(36)–C(35)	109.1(13)	B(4)–B(3)–B(8)	60.2(15)	B(5)–B(6)–B(7)	105.9(15)
C(13)–C(14)–C(15)	110.1(14)	B(5)–B(2)–B(1)	60.5(11)	B(7)–B(3)–B(8)	71.2(16)	B(10)–B(9)–B(4)	56.9(14)
C(14)–C(15)–C(16)	111.2(13)	B(5)–B(2)–B(6)	61.2(12)	B(1)–B(10)–B(5)	56.9(11)	B(4)–B(9)–B(8)	62.0(16)
C(11)–C(16)–C(15)	113.5(13)	B(1)–B(2)–B(3)	59.1(11)	B(1)–B(10)–B(4)	61.5(13)	B(8)–B(9)–B(10)	103.5(19)
P–C(21)–C(22)	111.2(10)	B(3)–B(2)–B(7)	59.0(12)	B(4)–B(10)–B(9)	55.3(13)	B(3)–B(8)–B(4)	62.0(15)
P–C(21)–C(26)	115.2(10)	B(7)–B(2)–B(6)	58.4(12)	B(9)–B(10)–B(5)	114.8(16)	B(4)–B(8)–B(9)	61.5(16)
		Au–B(5)–B(6)	69.4(10)			B(7)–B(8)–B(9)	114.0(19)

Table 4. Internuclear distances (Å) and interbond angles (°) in compound (**1b**)

Au–P	2.308(3)	B(3)–B(4)	1.765(23)	B(1)–B(2)	1.786(22)	B(2)–B(7)	1.726(22)
Au–B(5)	2.256(15)	B(4)–B(8)	1.783(23)	B(1)–B(3)	1.788(22)	B(3)–B(7)	1.790(22)
Au–B(6)	2.325(16)	B(4)–B(10)	1.838(23)	B(1)–B(4)	1.818(22)	B(3)–B(8)	1.765(23)
P–C(11)	1.822(7)	B(5)–B(10)	2.013(22)	B(1)–B(5)	1.776(22)	B(4)–B(9)	1.738(23)
P–C(21)	1.812(7)	B(8)–B(9)	1.779(24)	B(1)–B(10)	1.779(23)	B(5)–B(6)	1.745(22)
P–C(31)	1.819(7)	B(6)–B(7)	1.735(22)	B(2)–B(3)	1.767(22)	B(7)–B(8)	2.086(23)
C(12)–C(121)	1.532(14)	C(sol)–Cl(2a)	1.55(4)	B(2)–B(5)	1.745(21)	B(9)–B(10)	1.830(23)
C(22)–C(221)	1.545(14)	C(sol)–Cl(2b)	1.83(3)	B(2)–B(6)	1.677(22)	C(sol)–Cl(1)	1.79(3)
C(32)–C(321)	1.559(15)						

P–Au–B(5)	157.3(4)	C(23)–C(22)–C(221)	116.2(7)	B(1)–B(3)–B(4)	61.1(9)	B(2)–B(6)–B(7)	60.7(9)
P–Au–B(6)	157.3(4)	C(33)–C(32)–C(321)	117.9(7)	B(2)–B(3)–B(7)	58.0(9)	B(2)–B(7)–B(3)	60.3(9)
Au–P–C(11)	115.73(24)	C(31)–C(32)–C(321)	122.1(7)	B(4)–B(3)–B(8)	60.3(9)	B(2)–B(7)–B(6)	58.0(9)
Au–P–C(21)	111.09(24)	B(5)–Au–B(6)	44.8(5)	B(7)–B(3)–B(8)	71.8(9)	B(3)–B(7)–B(8)	53.53(79)
Au–P–C(31)	113.03(25)	B(2)–B(1)–B(3)	59.3(9)	B(1)–B(4)–B(3)	59.5(9)	B(3)–B(8)–B(4)	60.5(9)
P–C(11)–C(16)	117.6(5)	B(2)–B(1)–B(5)	58.6(9)	B(3)–B(4)–B(8)	59.3(9)	B(3)–B(8)–B(7)	54.64(81)
P–C(11)–C(12)	122.3(5)	B(3)–B(1)–B(4)	59.4(9)	B(8)–B(4)–B(9)	60.7(9)	B(4)–B(8)–B(9)	58.4(9)
P–C(21)–C(22)	121.4(5)	B(4)–B(1)–B(10)	61.4(9)	B(1)–B(4)–B(10)	58.2(9)	B(4)–B(9)–B(8)	60.9(9)
P–C(21)–C(26)	118.6(5)	B(5)–B(1)–B(10)	69.0(9)	B(9)–B(4)–B(10)	61.5(9)	B(4)–B(9)–B(10)	62.0(9)
P–C(31)–C(32)	121.2(5)	B(1)–B(2)–B(3)	60.4(9)	Au–B(5)–B(6)	69.7(7)	B(5)–B(10)–B(1)	55.45(81)
P–C(31)–C(36)	118.8(5)	B(1)–B(2)–B(5)	60.4(9)	B(1)–B(5)–B(2)	61.0(9)	B(1)–B(10)–B(4)	60.3(9)
C(11)–P–C(31)	104.7(3)	B(3)–B(2)–B(7)	61.7(9)	B(2)–B(5)–B(6)	57.5(9)	B(4)–B(10)–B(9)	56.6(9)
C(21)–P–C(31)	106.6(3)	B(5)–B(2)–B(6)	61.3(9)	B(1)–B(5)–B(10)	55.58(81)	B(6)–B(7)–B(8)	117.4(11)
C(11)–P–C(21)	105.0(3)	B(6)–B(2)–B(7)	61.3(9)	Au–B(5)–B(10)	87.33(72)	B(7)–B(8)–B(9)	113.2(11)
C(11)–C(12)–C(121)	123.4(7)	B(1)–B(3)–B(2)	60.3(9)	Au–B(6)–B(5)	65.5(7)	B(8)–B(9)–B(10)	105.4(11)
C(13)–C(12)–C(121)	116.5(7)	B(5)–B(10)–B(9)	118.5(11)	Au–B(6)–B(7)	132.9(10)	Cl(1)–C(sol)–Cl(2a)	96.2(16)
C(21)–C(22)–C(221)	123.8(7)			B(2)–B(6)–B(5)	61.3(9)	Cl(1)–C(sol)–Cl(2b)	105.5(14)

that each boron carries one terminal proton (all signals being doublets). A series of ^1H spectra with selective ^{11}B decoupling additionally showed which B resonances do not display coupling to bridge protons, namely those signals at $\delta(^{11}B)$ 8.34, 2.15, −30.7, and −35.8 p.p.m. Clearly, given the established decaborane-like structure of (**1b**) the only boron atoms with no direct connection to μ-H atoms are B(1), B(2), B(3), B(4), and B(5). Using the decaborane analogy further, it is reasonable to assume, on chemical shift grounds, that the two low-frequency signals in the boron spectrum derive from B(2) and B(4).

Table 5. Proposed boron assignments for compound (**1b**)

Assignment	$\delta(^{11}B)^a$	$\delta(^{1}H)^b$
6	15.13	5.27 (−3.3)
9	9.41	3.18 (−0.1, −2.8, −3.3)
3	8.34	3.66
1	2.15	3.10
7	1.40	3.67 (−0.1, −2.8, −3.3)
8,10	-1.00^c	2.64, 2.85 (−0.1, −2.8, −3.3)
5	-1.00^c	2.85 (−0.1, −2.8, −3.3)
2	−30.73	0.45
4	−35.85	0.51

[a] Relative to $BF_3{\cdot}OEt_2$ (external). [b] Relative to $SiMe_4$ from selective $^{1}H\text{-}\{^{11}B\}$ experiments. Chemical shifts of bridge protons enhanced by irradiation at ^{11}B frequencies shown in parentheses. [c] High- and low-frequency components of asymmetric singlet.

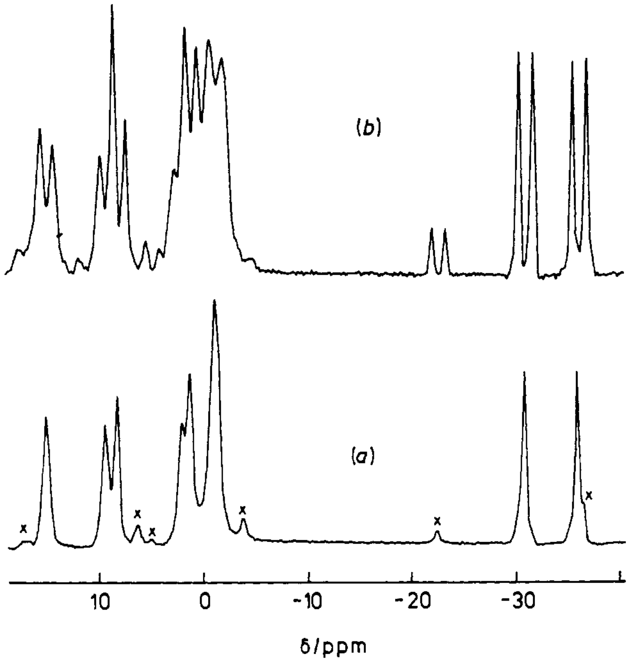

Figure 2. (*a*) $^{11}B\text{-}\{^{1}H\}$ and (*b*) ^{11}B n.m.r. spectra of compound (**1b**) obtained as a saturated solution in CD_2Cl_2 at 298 K. Peaks marked with a cross are due to a minor, unidentified impurity

Equally, on the basis of chemical shift together with the fact that it couples to only one bridging proton, the high-frequency signal at $\delta(^{11}B)$ 15.13 p.p.m. may be ascribed to B(6).

In order to derive more positive assignments for the ^{11}B (and hence the ^{1}H) signals, the ^{11}B(COSY) spectrum of (**1b**) was obtained (Figure 4). To summarise, the signal at $\delta(^{11}B)$ 15.13 p.p.m. displays coupling to those at 1.40 and −30.7 p.p.m. If our earlier assumptions are correct, then the signal at −30.7 p.p.m. is due to B(2), and by elimination that at −35.8 p.p.m. must arise from B(4). The signal at $\delta(^{11}B)$ 1.40 p.p.m., which shows coupling to that of B(6), also couples to that of B(2). Furthermore, it also shows bridge-H coupling, so it is probably due to B(7). This signal is also coupled to that at 8.34 p.p.m., and since the latter does not display coupling to a bridge proton, it must arise from B(3). The boron atom which resonates at δ 2.15 p.p.m. also has no μ-H attached, and since its signal couples to that of B(2) it must be due to B(1).

This leaves four boron atoms, 5, 8, 9, and 10, unaccounted for. Again, chemical shift arguments would suggest that B(9) gives rise to the signal at $\delta(^{11}B)$ 9.41, leaving the remaining three borons at −1.0 p.p.m. Even here some degree of resolution is possible, since close inspection of the COSY plot shows that the signal from B(4) has coupling to the higher-frequency component of the peak at −1.0 p.p.m. whilst the signal from B(2) couples to the lower-frequency part. This means that B(8) and B(10) resonate at slightly higher frequency than B(5). Unfortunately the coincidence between the former pair could not be resolved, although it may be noted that the selective $^{1}H\text{-}\{^{11}B\}$ spectra show that the protons terminal to B(8) and B(10) resonate at slightly different frequencies, specifically 2.85 and 2.64 p.p.m. Table 5 summarises the proposed boron assignments.

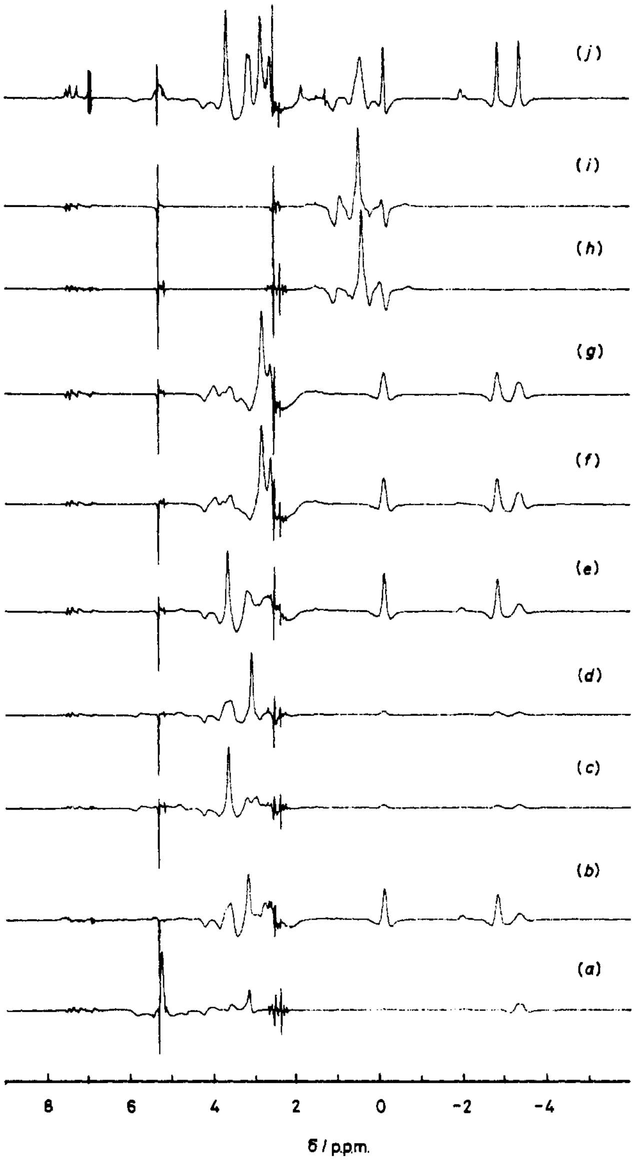

Figure 3. Traces (*a*)—(*i*) represent $^{1}H\text{-}\{^{11}B(\text{selective})\}$ n.m.r. results for compound (**1b**) presented as difference spectra by subtraction of an off-resonance decoupled spectrum from each of the $^{1}H\text{-}\{^{11}B(\text{selective})\}$ spectra. $\nu(^{11}B)$ correspond to $\delta(^{11}B)$ values of (*a*) 15.13, (*b*) 9.41, (*c*) 8.34, (*d*) 2.15, (*e*) 1.40, (*f*) −1.00 (high ν component), (*g*) −1.00 (low ν component), (*h*) −30.73, and (*i*) −35.85. Trace (*j*) represents a $^{1}H\text{-}\{^{11}B(\text{broad band})\}$ n.m.r. result, again presented as a difference spectrum

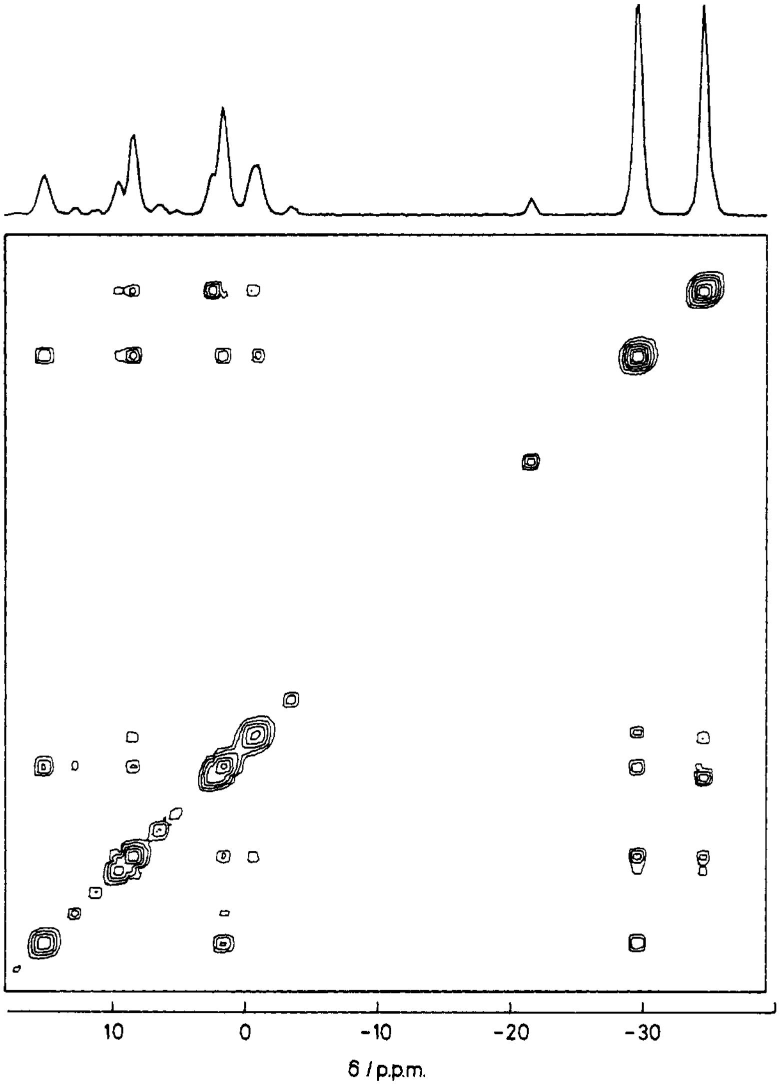

Figure 4. ^{11}B(COSY) plot for compound (**1b**) acquired overnight as a saturated solution in CD_2Cl_2, and transformed using a sine-bell squared function applied in both dimensions. The boron 90° pulse was 19 μs, and broad-band proton decoupling was applied throughout

Acknowledgements

We thank the S.E.R.C. for support, Dr. S. G. D. Henderson for some spectra, and the International Gold Corporation Ltd. for a generous loan of gold salts.

References

1 N. N. Greenwood and I. M. Ward, *Chem. Soc. Rev.*, 1974, **3**, 231.
2 N. N. Greenwood, *Pure Appl. Chem.*, 1977, **49**, 79; 1983, **55**, 77.
3 R. N. Grimes, in 'Comprehensive Organometallic Chemistry,' eds. G. Wilkinson, F. G. A. Stone, and E. W. Abel, Pergamon, Elmsford, 1982.
4 'Metal Interactions with Boron Clusters,' ed. R. N. Grimes, Plenum, New York, 1982, chs. 1—4, 6, and 7.
5 R. N. Grimes, *Acc. Chem. Res.*, 1983, **16**, 22.
6 J. D. Kennedy, *Prog. Inorg. Chem.*, 1984, **32**, 519; 1986, **34**, 211 and refs. therein.
7 N. N. Greenwood, *Chem. Soc. Rev.*, 1984, **13**, 353 and refs. therein.
8 L. F. Warren, jun., and M. F. Hawthorne, *J. Am. Chem. Soc.*, 1968, **90**, 4823.
9 S. J. Lippard and D. A. Ucko, *Inorg. Chem.*, 1968, **7**, 1051.
10 S. J. Lippard and K. M. Melmed, *Inorg. Chem.*, 1969, **8**, 2755.
11 E. L. Muetterties, W. G. Peet, P. A. Wegner, and C. W. Alegranti, *Inorg. Chem.*, 1970, **9**, 2447.
12 J. T. Gill and S. J. Lippard, *Inorg. Chem.*, 1975, **14**, 751.
13 H. M. Colquhoun, T. J. Greenhough, and M. G. H. Wallbridge, *J. Chem. Soc., Chem. Commun.*, 1976, 1019; *J. Chem. Soc., Dalton Trans.*, 1978, 303; *Acta Crystallogr., Sect. B*, 1977, **33**, 3604; *J. Chem. Soc., Chem. Commun.*, 1980, 192.
14 M. A. Beckett, J. E. Crook, N. N. Greenwood, and J. D. Kennedy, *J. Chem. Soc., Dalton Trans.*, 1984, 1427.
15 V. T. Brice and S. G. Shore, *J. Chem. Soc., Dalton Trans.*, 1975, 334.
16 C. G. Outterson, V. T. Brice, and S. G. Shore, *Inorg. Chem.*, 1976, **15**, 1456.
17 N. N. Greenwood, J. A. Howard, and W. S. McDonald, *J. Chem. Soc., Dalton Trans.*, 1977, 37.
18 N. N. Greenwood and J. T. Staves, *J. Chem. Soc., Dalton Trans.*, 1978, 1144.
19 G. K. Barker, N. R. Godfrey, M. Green, H. E. Parge, F. G. A. Stone, and A. J. Welch, *J. Chem. Soc., Chem. Commun.*, 1983, 277.
20 N. W. Alcock, L. Parkhill, and M. G. H. Wallbridge, *Acta Crystallogr., Sect. C*, 1985, **41**, 716.
21 Ref. 4, ch. 5.
22 C. R. Peters and C. E. Nordman, *J. Am. Chem. Soc.*, 1960, **82**, 5758.
23 G. F. Mitchell and A. J. Welch, *J. Chem. Soc., Dalton Trans.*, 1987, 1017.

24 R. D. Dobrott and W. N. Lipscomb, *J. Chem. Phys.*, 1962, **37**, 1779.
25 M. Brookhart and M. L. H. Green, *J. Organomet. Chem.*, 1983, **250**, 395.
26 R. Hoffmann, *Angew. Chem., Int. Ed. Engl.*, 1982, **21**, 771 and refs therein.
27 See, for example, L. W. Bateman, M. Green, K. A. Mead, R. M. Mills, I. D. Salter, F. G. A. Stone, and P. Woodward, *J. Chem. Soc., Dalton Trans.*, 1983, 2599.
28 K. Wade, *Chem. Commun.*, 1971, 792.
29 L. Barton, *Top. Curr. Chem.*, 1982, **100**, 169.
30 A. J. Wynd, S. E. Robins, D. A. Welch, and A. J. Welch, *J. Chem. Soc., Chem. Commun.*, 1985, 819.
31 G. B. Jacobsen, D. G. Meina, J. H. Morris, C. Thomson, S. J. Andrews, D. Reed, A. J. Welch, and D. F. Gaines, *J. Chem. Soc., Dalton Trans.*, 1985, 1645.
32 J. A. Muir, M. M. Muir, L. B. Pulgar, P. G. Jones, and G. M. Sheldrick, *Acta Crystallogr., Sect. C*, 1985, **41**, 1174.
33 B. J. Gregory and C. K. Ingold, *J. Chem. Soc. B*, 1969, 276.
34 A. J. Carty and A. Efraty, *Inorg. Chem.*, 1969, **8**, 543.
35 G. Calvin, G. E. Coates, and P. S. Dixon, *Chem. Ind. (London.)*, 1959, 1628.
36 M. F. Hawthorne, A. R. Pitochelli, R. D. Strahm, and J. J. Miller, *J. Am. Chem. Soc.*, 1960, **82**, 1825.
37 N. G. Walker and D. Stuart, *Acta Crystallogr., Sect. A*, 1983, **39**, 158.
38 International Tables for *X*-Ray Crystallography, Kynoch Press, Birmingham, 1974, vol. 4, 99.
39 G. M. Sheldrick, University of Cambridge, 1976.
40 R. O. Gould and D. E. Smith, University of Edinburgh, 1986.
41 R. O. Gould and P. Taylor, University of Edinburgh, 1986.
42 C. K. Johnson, Report ORNL 5138, Oak Ridge National Laboratory, Tennessee, 1976.
43 G. M. Sheldrick, University of Göttingen, 1986.
44 A. J. Wynd and A. J. Welch, *J. Chem. Soc., Chem. Commun.*, 1987, 1174; A. J. McLennan, A. J. Wynd, and A. J. Welch, unpublished work.
45 N. N. Greenwood, J. A. McGinnety, and J. D. Owen, *J. Chem. Soc., Dalton Trans.*, 1972, 989.
46 C. A. Tolman, *Chem. Rev.*, 1977, **77**, 413.
47 G. K. Barker, M. Green, F. G. A. Stone, A. J. Welch, T. P. Onak, and G. Siwapanyoyos, *J. Chem. Soc., Dalton Trans.*, 1979, 1687.
48 M. Green, A. G. Orpen, I. D. Salter, and F. G. A. Stone, *J. Chem. Soc., Dalton Trans.*, 1984, 2497.
49 H. Lehner, D. Matt, P. S. Pregosin, L. M. Venanzi, and A. Albinati, *J. Am. Chem. Soc.*, 1982, **104**, 6825.
50 G. Schmid, R. Pfeil, R. Boese, F. Bandermann, S. Meyer, G. H. M. Calis, and J. A. W. van der Velden, *Chem. Ber.*, 1981, **11**, 4634.
51 R. Brill, H. Dietrich, and H. Dierks, *Acta Crystallogr., Sect. B*, 1971, **27**, 2003.

Received 12*th December* 1986; *Paper* 6/2395